

Global Properties in an Experimental Realization of Time-Delayed Feedback Control with an Unstable Control Loop

Klaus Höhne, Hiroyuki Shirahama, Chol-Ung Choe, and Hartmut Benner

Institute for Solid State Physics, Darmstadt University of Technology, Hochschulstraße 6, D-64289 Darmstadt, Germany

Kestutis Pyragas

Semiconductor Physics Institute, A. Gostauto 11, LT-01108 Vilnius, Lithuania

Wolfram Just*

Queen Mary / University of London, School of Mathematical Sciences, Mile End Road, London E1 4NS, United Kingdom

(Received 9 January 2007; published 25 May 2007)

We demonstrate by electronic circuit experiments the feasibility of an unstable control loop to stabilize torsion-free orbits by time-delayed feedback control. Corresponding analytical normal form calculations and numerical simulations reveal a severe dependence of the basin of attraction on the particular coupling scheme of the control force. Such theoretical predictions are confirmed by the experiments and emphasize the importance of the coupling scheme for the global control performance.

DOI: [10.1103/PhysRevLett.98.214102](https://doi.org/10.1103/PhysRevLett.98.214102)

PACS numbers: 05.45.Gg, 02.30.Ks, 07.05.Dz

Introduction.—Time-delayed feedback control was invented in the early 1990s [1] as a simple, robust, and efficient method to control unstable time periodic orbits in chaotic systems (cf. [2] for a recent overview of topics in control of chaos). Early analytical investigations indicated that unstable orbits with an odd number of real unstable modes cannot be stabilized by time-delayed feedback control [3]. Roughly speaking, this means that torsion of the unstable modes is necessary so that an orbit becomes accessible to time-delayed feedback control [4]. While it has been shown recently that such a constraint does not apply to autonomous systems because of symmetries induced by time translation invariance [5], the so called odd-number limitation still applies to the frequently used setup of periodically driven systems. To overcome this limitation, the counterintuitive idea of an unstable control loop has been proposed [6,7]. By including an additional unstable mode into the control loop, one artificially enlarges the set of real multipliers greater than unity to an even number. While this concept has been successfully applied in numerical simulations, an experimental verification is still missing even for very simple experimental setups.

Analytical approaches for time-delayed feedback control have been mostly based on linear stability analysis since such a method can predict the success of the control without resorting to details of the underlying dynamical system [4]. But even if such an analysis predicts stable states, experimental success is not guaranteed because the control performance may severely depend on the basin of attraction of the stabilized state. Such a global feature of time-delay dynamics is difficult to evaluate, in particular, when the underlying equations of motion are unknown. But recently, a simple generic mechanism based on bifurcation theory has proven its relevance in determining the size of basins in time-delayed feedback control experiments [8].

We will show that the straightforward experimental implementation of an unstable controller may be hampered by small basins. Our analysis will point out that basins can be enlarged considerably by coupling control forces through the phase of the signal. We will supply analytical estimates, numerical evidence, and experimental results. Since the quantitative detection of basins requires well-defined initial conditions for the whole time-delay system, the experimental approach will rely on demonstration experiments in terms of electronic circuits.

Theoretical considerations.—As a generic model for a nonlinear oscillator with an unstable limit cycle, let us consider the normal form of a subcritical Hopf bifurcation. The complex valued variable z_t describes the oscillator, and the equations of motion subjected to time-delayed feedback control read

$$\dot{z}_t = \{-\lambda + i\omega + |z_t|^2\}z_t + w_t z_t g(|z_t|) \quad (1a)$$

$$\dot{w}_t = \alpha w_t - K(|z_t| - |z_{t-\tau}|)|z_t|g(|z_t|). \quad (1b)$$

The control force is governed by the real variable w_t , and the choice $\alpha > 0$ corresponds to an unstable control loop. In addition, we allow for different types of coupling of the control force which is governed by the function g . Here, we assume $\lambda > 0$ and $\omega > 0$ so that Eqs. (1) admit an unstable harmonic limit cycle $z_t = r_* \exp(i\omega t)$ with amplitude $r_* = \sqrt{\lambda}$ if the delay is adjusted accordingly, i.e., $\tau = 2\pi/\omega$. Although Eqs. (1) might look quite tedious, they can be considered as some type of minimal model which can be derived, for instance, close to a subcritical Hopf instability $|\lambda| \ll |\omega|$ by averaging methods. Thus, Eqs. (1) may be regarded as a generic model for studying the dependence of the control performance on the choice of the coupling. In particular, it has been suggested in [9] that for the use of the unstable controller, a linear contribution in the coupling is

essential to ensure sufficient coupling between the control device and the dynamical degrees of freedom.

Using polar coordinates $z_t = r_t \exp(i\phi_t)$ and approximating the time-delayed difference by a derivative $|z_t| - |z_{t-\tau}| \simeq \tau \dot{r}_t$, which is consistent within the spirit of an averaging approach, the system (1) may be reduced to a two-dimensional differential equation

$$\dot{r}_t = (-\lambda + r_t^2)r_t + w_t r_t g(r_t) \quad (2a)$$

$$\dot{w}_t = \alpha w_t - K \tau \dot{r}_t r_t g(r_t). \quad (2b)$$

The limit cycle of interest is determined by the nontrivial fixed point $r_* = \sqrt{\lambda}$, $w_* = 0$. In order to study the influence of the coupling function g on the control performance, we focus on two special limiting cases: namely, $g(r) \equiv 1$ and $rg(r) \equiv 1$, respectively.

The case $g(r) \equiv 1$ has been actually considered in [9] to illustrate the idea of the unstable controller in a mathematical model system. Applying linear stability analysis to Eqs. (2), one obtains an interval of control amplitudes such that the nontrivial fixed point becomes stable. The lower boundary of this interval is given by the critical control amplitude $K_c = (2\lambda + \alpha)/(\tau\lambda)$. At such a value, control sets in through a Hopf bifurcation. An analysis beyond linear stability in terms of normal forms reveals that the Hopf bifurcation is degenerate since the third order nonlinear coefficient is imaginary. Thus, the system is sensitive to small perturbations, and finally subcritical behavior may prevail, yielding a mechanism which causes small basins (cf. e.g., [10]).

A change of the coupling function g may change the nature of the instability at the control threshold. For instance, if we employ $rg(r) \equiv 1$ and follow the steps described in the previous paragraph, we again obtain a control interval with lower boundary $K_c = (2\lambda + \alpha)/\tau$. Now the bifurcation at that threshold turns out to be supercritical; i.e., stable oscillations around the target state are observed below the control threshold and stabilization sets in for $K > K_c$. The transition is continuous, and the basin of the controlled state stays large even close to the control threshold. The choice $rg(r) \equiv 1$ is actually a limiting case as the coupling function becomes singular at the origin. But it means that the coupling in Eq. (1) appears through the phase of the variable only, without any dependence on the amplitude. Our considerations suggest that with such a choice, the basin of the target state can be increased and that such a recipe applies to a general class of nonlinear oscillators.

Numerical simulations.—We first confirm the general theoretical considerations by numerical simulations of the van der Pol equations [11]

$$\dot{x}_t = -y_t + \varepsilon x_t + x_t^3/3 + w_t G(x_t) \quad (3a)$$

$$\dot{y}_t = x_t \quad (3b)$$

$$\dot{w}_t = \alpha w_t - K(x_t - x_{t-\tau})G(x_t). \quad (3c)$$

For $\varepsilon < 0$, the model admits an unstable limit cycle. The

choice $G(x) = x$ for the coupling function yields the model already discussed in [9]. Stabilization of the unstable state is possible for small values of α and $|\varepsilon|$. Actually, for $|\varepsilon| \ll 1$, averaging yields essentially Eq. (2) where the coupling functions are related via $rg(r) \sim \int_0^{2\pi} \cos\varphi G(r \cos\varphi) d\varphi$, up to some numerical factor. Thus, the linear coupling $G(x) = x$ is expected to suffer from small basins of attraction while a sigmoidal choice should yield increased basins and a related improvement of the control performance. Here, we consider parameter values $\varepsilon = -0.1$, $\alpha = 0.1$ and compare results for two different coupling functions, $G(x) = x$ and $G(x) = \tanh(10x)$. Stabilization of the periodic orbit with period $\tau = 6.2871\dots$ is observed in the control intervals $K \in [0.4, 0.6]$ and $K \in [0.1, 0.15]$, respectively.

To visualize global properties of time-delayed feedback control, like basins of attraction of the stabilized state, one has to cope with the infinite-dimensional phase space of time-delay dynamics. Here, we fix initial conditions on a two-dimensional cross section in such a way that for given initial coordinates (x_0, y_0) , the time-delayed feedback control device is switched off for one period τ . Thus, the history is taken from the uncontrolled dynamics and is solely determined by the two-dimensional initial coordinate. Initial conditions for which control works successfully are then displayed in a diagram. Such an approach which has been already proposed for the theoretical analysis of time-delayed feedback control [12] will be applied for simulations and for experimental data.

The corresponding two-dimensional cross sections of the basins are displayed in Fig. 1 for the two choices of couplings, a linear coupling $G(x) = x$ and a sigmoidal choice $G(x) = \tanh(10x)$. Close to the control threshold, the linear coupling function generates a fairly small basin of attraction, in accordance with subcritical behavior. No such limitation occurs for the sigmoidal coupling where the basin stays large even close to the control threshold. Even deep within the control interval, the basin remains fairly small for the linear choice, compared to the sigmoidal coupling. Overall, a pronounced improvement of the control performance is observed when the coupling is chosen appropriately, i.e., when the sign of the signal is used to determine the control force. Thus, our findings are in complete agreement with the previous general theoretical considerations.

Experimental setup and results.—We finally apply the concept of an unstable controller to an experimental situation where, e.g., insufficient sensitivity, mismatched or drifting parameters, internal offsets, and noise may severely hamper the control performance. We designed an autonomous electronic circuit along the lines of Eq. (3). A block diagram of this setup is shown in Fig. 2. Besides the van der Pol oscillator circuit, the diagram includes the unstable controller as well as elements for defining the experimental initial condition. The components at the top of Fig. 2 map the relation $\dot{y} = x$. Then, by integrating x the

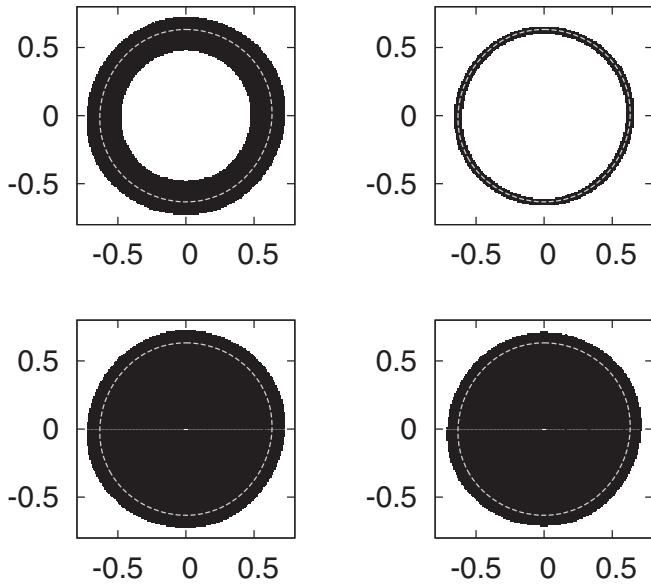


FIG. 1. Two-dimensional cross section of the basin of Eq. (3) for linear coupling function $G(x) = x$ (top) and sigmoidal coupling function $G(x) = \tanh(10x)$ (bottom) at $\varepsilon = -0.1$ and $\alpha = 0.1$. Left: basin deep inside the control domain at $K = 0.5$ (left, top) and $K = 0.125$ (left, bottom). Right: basin close to the control threshold at $K = 0.405$ (right, top) and $K = 0.105$ (right, bottom). The broken line indicates the stable target state.

variable y is obtained. The adder comprehends all terms contributing to \dot{x} , and x is again obtained by integration. The controller variable w is coupled to the x -component, so the product of w and $G(x)$ is also included in the inputs of the adder, while the delay term and the intrinsic instability of w are generated by the loops at the bottom of the diagram. The bifurcation parameter ε , the control amplitude K , and the positive exponent α are determined by the gain of electronic amplifiers. It turned out that small internal offset voltages at the electronic multipliers could affect the size, symmetry, and position of the target orbit. For defining the initial conditions, we introduced switches parallel to each of the integrator outputs which generate the variables x_t , y_t , and w_t . These switches allowed to apply adjustable constant voltages x_0 , y_0 , and w_0 , respectively. Thus, when switching on the system at $t = 0$, the variables x_t and y_t start from a well-defined state. At about two cycles later, the feedback loop which generates the control signal and the controller variable w_t is switched on. Such a time lag is necessary to fill the memory with the history of the uncontrolled dynamics.

Our experimental results underline that the success of control depends sensitively on the specific form of the coupling function $G(x)$. When applying a linear coupling $G(x) = x$ successful control was obtained only for a small range of initial conditions close to the target orbit, as expected from our numerical simulations. Starting from initial conditions outside this small range, the controller variable w_t immediately escaped to infinity while x_t and y_t , after some irregular transient, either approached the center

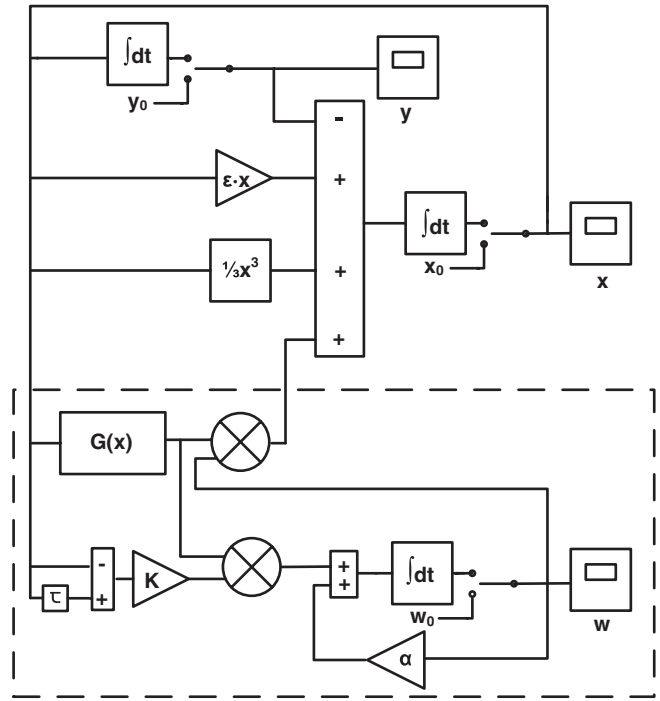


FIG. 2. Block diagram of the van der Pol oscillator with control loop.

of the orbit or ended up in some high amplitude oscillatory state which meets the saturation limits of the operational amplifiers. Close to the target orbit, however, the control mechanism worked successfully. Switching on the feedback loop at $t = 2$ ms w_t first shows a distinct pulse and then settles close to 0 V, while the measured signal y_t oscillates with increasing amplitude and settles at the target orbit (cf. Fig. 3). This observation, in fact, represents the first experimental evidence approving the concept of an unstable controller in general.

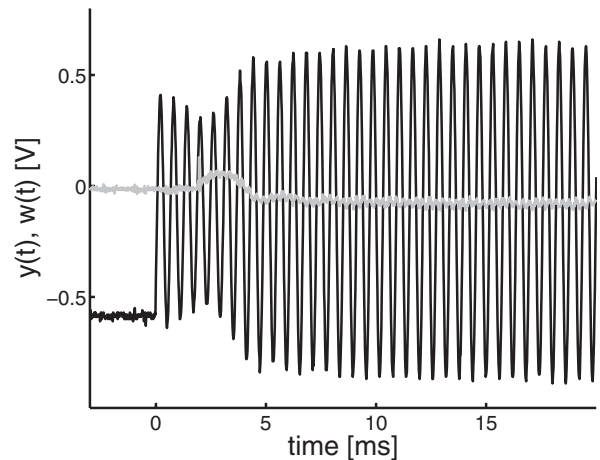


FIG. 3. Successful control of a torsion-free unstable orbit with period $\tau = 0.57$ ms using $G(x) = x$, $\varepsilon = -0.1$, $K = 0.4$, and initial conditions $x_0 = w_0 = 0$ V and $y_0 = -0.55$ V. Grey: control variable w_t , black: measured signal y_t .

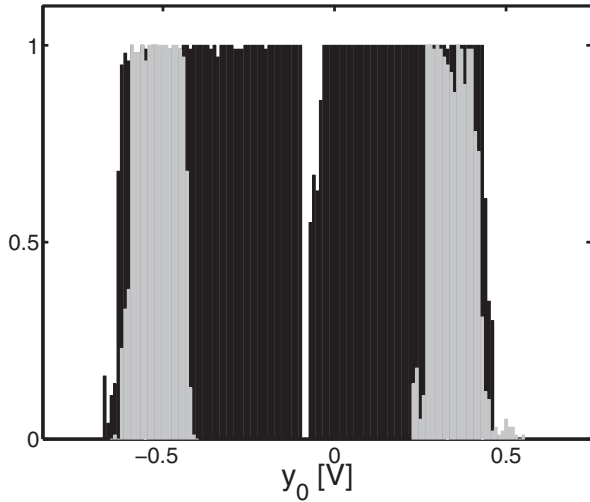


FIG. 4. Experimentally obtained histograms for successful control in dependence on the initial condition y_0 for different control couplings and $\varepsilon = -0.1$, $x_0 = w_0 = 0$ V. Grey: linear coupling $G(x) = x$ ($K = 0.4$), black: sigmoidal coupling $G(x) = \text{sgn}(x)$ ($K = 0.15$).

When replacing the linear coupling $G(x) = x$ by a sigmoidal one, e.g., $G(x) = \text{sgn}(x)$ or $G(x) = \tanh(\beta x)$, $\beta \gg 1$, the situation changed considerably. Technically, such a modification of the coupling could be easily implemented by means of an operational amplifier acting as a comparator. After such an implementation, the control performance improves considerably.

A quantitative estimate of the control performance was obtained by varying both the control amplitude and the initial conditions at a fixed value of $\varepsilon = -0.1$. In the case of linear coupling, control was achieved in the range $K \in [0.28, 0.67]$ with shortest transient behavior at about $K = 0.4$ while for the sigmoidal case, control was observed in the range $K \in [0.12, 0.16]$. We fixed initial conditions x_0 and w_0 at zero and changed y_0 from -0.8 V to $+0.8$ V in steps of 10 mV. For each set of initial values, we repeated the control experiment about 100 times. The fraction of successful attempts is shown in a histogram, Fig. 4, in dependence of y_0 . For linear coupling, successful control was merely achieved for values of y_0 slightly below the radius of the unstable orbit. We observe in addition a slight asymmetry which is caused by the offset at the respective multiplier. For the sigmoidal coupling, the “basin of attraction” of the controlled orbit was found to be much larger than in the linear case. Apart from a narrow gap at the center, the basin now covers the full range of y_0 inside the orbit.

Conclusion.—We have studied in detail the implementation of an unstable controller to stabilize periodic orbits with a single real unstable Floquet mode by time-delayed feedback control. Our setup provides the first experimental proof of the feasibility of such a concept. We therefore conclude that unstable controllers are a suitable tool to broaden the scope of time-delayed feedback techniques.

Furthermore, our analysis highlights the importance of suitable coupling schemes to improve the overall control performance, in particular, with regards to basins of attraction. By using the phase information of the measured signal, one is able to enlarge the basins of attraction considerably since the corresponding instabilities at the control boundaries become supercritical. Our conclusions have been supported by analytical considerations, numerical evidence, and experimental results.

Our analysis has shown that one can even cope with infinite-dimensional phase spaces of delay systems in real experiments when appropriate cross sections are considered. Thus, even features beyond linear stability properties can be addressed whenever the experimental setup allows for reproducible initial conditions of the time-delay dynamics, like in our electronic circuit setup. In such a respect, investigations of time-delayed feedback control have a wider scope and may even contribute to fundamental aspects of general time-delay dynamics.

The experimental study is still in progress, and further systematic investigations of global properties are necessary. Even now, it is already clear that in systems without torsion the idea of the unstable controller does work and, for an appropriate type of coupling, time-delayed feedback control becomes suitable for practical applications. In particular, it is tempting to compare the efficiency of different strategies for controlling such orbits, like unstable controllers, rhythmic control [13], and the implementation of recent results for autonomous systems [5].

Financial support by the Humboldt Foundation and by Deutsche Forschungsgemeinschaft (Grant No. BE 864/4-3) is gratefully acknowledged.

*Electronic address: w.just@qmul.ac.uk

- [1] K. Pyragas, Phys. Lett. A **170**, 421 (1992).
- [2] *Handbook of Chaos Control*, edited by H.G. Schuster (Wiley-VCH, Berlin, 1999).
- [3] H. Nakajima, Phys. Lett. A **232**, 207 (1997).
- [4] W. Just, T. Bernard, M. Ostheimer, E. Reibold, and H. Benner, Phys. Rev. Lett. **78**, 203 (1997).
- [5] B. Fiedler, V. Flunkert, M. Georgi, P. Hövel, and E. Schöll, Phys. Rev. Lett. **98**, 114101 (2007).
- [6] K. Pyragas, Phys. Rev. Lett. **86**, 2265 (2001).
- [7] V. Pyragas and K. Pyragas, Phys. Rev. E **73**, 036215 (2006).
- [8] C. v. Loewenich, H. Benner, and W. Just, Phys. Rev. Lett. **93**, 174101 (2004).
- [9] K. Pyragas, V. Pyragas, and H. Benner, Phys. Rev. E **70**, 056222 (2004).
- [10] W. Just, H. Benner, and C.V. Loewenich, Physica D (Amsterdam) **199**, 33 (2004).
- [11] B. van der Pol, Philos. Mag. **2**, 978 (1926).
- [12] K. Yamasue and T. Hikihara, Phys. Rev. E **69**, 056209 (2004).
- [13] H.G. Schuster and M.B. Stemmler, Phys. Rev. E **56**, 6410 (1997).